Structure of Si(001) surfaces. I. The origin of the buckling in the dimer formation on reconstructed surfaces

M. Tsuda
Laboratory of Physical Chemistry, Faculty of Pharmaceutical Sciences, Chiba University, Chiba 260, Japan

T. Hoshino
School of Science and Engineering, Waseda University, 3-4-1 Ohkubo, Shinjuku-ku, Tokyo 169, Japan

S. Oikawa
Laboratory of Physical Chemistry, Faculty of Pharmaceutical Sciences, Chiba University, Chiba 260, Japan

I. Ohdomari
School of Sciences and Engineering, Waseda University, 3-4-1 Ohkubo, Shinjuku-ku, Tokyo 169, Japan
(Received 27 February 1991)

The buckling mechanism of dimers on reconstructed Si(001) surfaces was investigated by *ab initio* Hartree-Fock molecular-orbital calculations in the electrically neutral, negatively charged, and positively charged cases. The energy-minimized geometries of dimers depend upon their electrical charge: The most stable geometry is symmetric for the electrically neutral case, but asymmetric or buckled for the negatively and positively charged cases. These results reveal the origin of the buckling in the dimer formation to be an imbalance of the electrical charges on the Si(001) surface. The electronic structure has the remarkable feature that an unpaired electron is localized on one side of the top Si atoms in a buckled dimer. These theoretical results are found to be consistent with those of recent scanning-tunneling-microscopy experiments.

I. INTRODUCTION

Surface reconstructions on (001) planes of silicon crystals have been studied by many experimental and theoretical physicists.[1–16] Analyses by low-energy electron diffraction (LEED) (Refs. 1–3) show that the surface is reconstructed to a (2×1) or $c(4\times2)$ structure. An experiment[4] with He diffraction suggests that $p(2\times2)$ and possibly $c(2\times2)$ regions also exist on the reconstructed surface in addition to the (2×1) and $c(4\times2)$ structures.

Chadi[5] carried out energy-minimization calculations using a semiempirical tight-binding method[6] and obtained the result that a buckled dimer was more stable than a nonbuckled dimer in the (2×1) structure. Total-energy calculations using an *ab initio* self-consistent pseudopotential approach by Yin and Cohen[7] and a semiempirical cluster method by Verwoerd[8] came to the same conclusion. Chadi also indicated that the energy-band structure of the asymmetric surface is semiconducting as shown by experiments of angle-resolved ultraviolet photoemission spectroscopy (ARUPS) (Refs. 9–11) and photoelectron spectroscopy.[12]

Contrary to Chadi's results, Artacho and Yndurain[13] recently found that an inclusion of a spin arrangement to the total-energy calculation causes a nonbuckled dimer to be more stable than a buckled one and the energy-band structure of the symmetric surface is also semiconducting. Furthermore, Redondo and Goddard[14] reported that the inclusion of proper electron correlation produces a symmetric dimer description and its ionization potential is consistent with the experimental results.

Observation of the Si(001) surface by scanning tunneling microscopy (STM) (Refs. 15–17) yielded definite information on the buckling: Dimers are not buckled on a complete and flat terrace, whereas dimer rows have a zigzag shape in the vicinity of a dimer defect. Furthermore, dimers at a step edge are buckled. These findings revealed that the nonbuckled dimers and the buckled dimers coexist on the same Si(001) surface, and the formation of buckled dimers is favored at nonuniform parts of the surface whereas that of the nonbuckled dimers is favored at uniform parts.

These STM observations cannot be explained clearly if we still resort to simply comparing the total energies between the buckled and the nonbuckled dimers, as many theoreticians used to do. There must exist a principal origin that causes the buckling of dimers on the Si(001) surface. This paper describes a theoretical approach to this problem.

Si(001) surfaces have many defects, steps, and possibly accidental contaminants, all of which cause nonuniform electrical charge distributions on the surface. For this reason, the positively or negatively charged parts will exist on the surface along with the electrically neutral places.

We investigated the most stable atomic configurations and the electronic structures of Si(001) surfaces in the charged and noncharged cases one by one using a model molecular system. The quantum chemical calculation results explain well the origin of the buckling of dimers on Si(001) surfaces: The buckling comes from an imbalance of the electric charge distribution on the surface.

II. METHOD OF CALCULATION

A. Computational procedure

The atomic configuration and the electronic structure of a molecular system are completely determined and described by the quantum chemical method.[18] The total energy E of a molecular system comprising N electrons and ν nuclei is given as an eigenvalue of the Schrödinger equation (1), where Ψ is the corresponding eigenstate function described by position vectors of N electrons and ν nuclei.

$$H\Psi=E\Psi \ , \tag{1}$$

where

$$\Psi=\Psi(x_1,y_1,z_1,\xi_1,\ldots,x_i,y_i,z_i,\xi_i,\ldots,x_N,y_N,z_N,\xi_N,X_1,Y_1,Z_1,\Xi_1,\ldots,X_\alpha,Y_\alpha,Z_\alpha,\Xi_\alpha,\ldots,X_\nu,Y_\nu,Z_\nu,\Xi_\nu) \ ,$$

$$H=-\frac{\hbar^2}{2m}\sum_{i=1}^{N}\left[\frac{\partial^2}{\partial x_i^2}+\frac{\partial^2}{\partial y_i^2}+\frac{\partial^2}{\partial z_i^2}\right]-\frac{\hbar^2}{2}\sum_{\alpha=1}^{\nu}\frac{1}{M_\alpha}\left[\frac{\partial^2}{\partial X_\alpha^2}+\frac{\partial^2}{\partial Y_\alpha^2}+\frac{\partial^2}{\partial Z_\alpha^2}\right]$$
$$-\sum_{\alpha=1}^{\nu}\sum_{i=1}^{N}\frac{Z_\alpha e^2}{|\mathbf{R}_\alpha-\mathbf{r}_i|}+\frac{1}{2}\sum_{i=1}^{N}\sum_{\substack{j=1\\(j\neq i)}}^{N}\frac{e^2}{|\mathbf{r}_i-\mathbf{r}_j|}+\frac{1}{2}\sum_{\alpha=1}^{\nu}\sum_{\substack{\beta=1\\(\beta\neq\alpha)}}^{\nu}\frac{Z_\alpha Z_\beta e^2}{|\mathbf{R}_\alpha-\mathbf{R}_\beta|} \ ,$$

$$|\mathbf{R}_\alpha|=(X_\alpha^2+Y_\alpha^2+Z_\alpha^2)^{1/2} \ ,$$

$$|\mathbf{r}_i|=(x_i^2+y_i^2+x_i^2)^{1/2} \ ,$$

where x_i,y_i,z_i and $X_\alpha,Y_\alpha,Z_\alpha$ are the position coordinates of the ith electron and the αth nucleus, respectively. ξ_i and Ξ_α are the spin coordinates in the same manner. m and M_α are the mass of an electron and the αth nucleus; $-e$ and $Z_\alpha e$ are the charges of an electron and the αth nucleus, respectively.

Equation (1) is separated analytically under the Born-Oppenheimer adiabatic approximation into two eigenvalue equations; i.e., one is the equation on the electronic state where independent valuables are the coordinates of electrons, x_i, y_i, z_i, and ξ_i, whereas the other is the equation whose independent valuables are the coordinates of nuclei, X_α, Y_α, Z_α, and Ξ_α. The eigenstate function Ψ is a simple product of an electronic state function $\Psi_{\text{elec}}(r,R)$ obtained from the former equation and a nuclear state function $\Psi_{\text{nucl}}(R)$ arisen from the latter equation.

$$\Psi=\Psi_{\text{elec}}(r,R)\Psi_{\text{nucl}}(R) \ . \tag{2}$$

The coordinates of nuclei R in $\Psi_{\text{elec}}(r,R)$ are parameters that express the molecular structure. The energy eigenvalue of the corresponding electronic state function Ψ_{elec} is the potential energy of the molecular structure determined by the parameter R in the electronic state.

The electronic state function $\Psi_{\text{elec}}(r,R)$ and its energy eigenvalue were obtained by an *ab initio* molecular-orbital (MO) method under the Hartree-Fock (HF) approximation; i.e., the electronic state function Ψ_{elec} is expressed by one Slater determinant constructed from spin-adopted MO's. Restricted HF functions were used for the spin-singlet electronic states whereas unrestricted HF functions were used for the spin-doublet and spin-triplet states.

In the *ab initio* MO method, a MO function is a linear combination of Gaussian basis-set functions whose origins are on each atom expressed by the basis-set function. Since the model molecular system used in this paper is too large for the usual *ab initio* calculations, the effective core potential method proposed by Wadt and Hay[19] was used. In this method, MO functions are described by a linear combination of basis-set functions which expresses $3s$ and $3p$ valence atomic orbitals (AO's) of Si atoms and $1s$ AO's of H atoms; i.e., each AO is a contracted function comprised of three Gaussians, except the $3s$ and $3p$ AO's of the top Si atoms which form a dimer on the surface. For these AO's of the top Si atoms, one contracted function was split into two functions; i.e., one Gaussian and a contracted function made from two Gaussians. Furthermore, we added to those top Si atoms a set of Rydberg AO's (Ref. 20) [one s-type ($\alpha=0.017$) and three p-type AO's ($\alpha=0.017$)] to describe accurately the spatial distribution of electrons of the surface atoms.

The stable structure of a molecular system can be determined as the minimum on the $(3\nu-6)$-dimensional potential-energy hypersurface, where ν is the number of nuclei of the molecular system. The minimum was found by the energy gradient method under the condition that all the gradients are zero, i.e.,

$$\partial E(q_1,q_2,\ldots,q_r,\ldots,q_{3\nu-6})/\partial q_r=0 \ , \quad r=1,2,\ldots,3\nu-6 \ , \tag{3}$$

where q_r is the rth internal coordinate of the molecule. In order to describe a crystal structure simply, atoms of the underlayers were fixed at the initial positions. In such a case, the internal coordinates of these fixed atoms are omitted from Eq. (3).

The program used in the calculations is the IMS (Institute for Molecular Science, Okazaki, Japan) version of GAUSSIAN82 (Ref. 21) for the geometry optimization and various analyses on the electronic structure.

B. Model molecular system

Figure 1(a) represents the unreconstructed Si(001)-(1×1) surface. Two Si atoms in the top layer will approach each other to form a buckled dimer or a nonbuckled one. The nature of these two Si atoms is considered to be a major factor in the cause of this reconstruction.

In order to describe the reconstruction process of the Si(001) surface, we must note the two top Si atoms denoted as solid spheres in Fig. 1(a). The first, second, and third underlayers also have to be considered. For these reasons, the construction of the smallest model molecular system for calculations was performed in the following way: the Si atoms designated by the solid spheres in Fig. 1(a) remained and those designated by the open spheres were replaced by hydrogen atoms. Consequently, a Si_9H_{12} model was obtained. This model is formed in a different way from the adamantane structure shown in Fig. 1(c) when some top atoms, denoted as open circles, are removed. The energy-minimized geometry of the adamantane has the same bond angles and longer bond lengths by 0.11 Å compared with those of *c*-Si. We used the structure [Fig. 1(b)] produced from the optimized structure of the adamantane as a model of the Si(001) surface in the calculations.

The calculations were carried out in the following three cases.

(1) The dimer is electrically neutral (the spin-singlet and spin-triplet states).

(2) The dimer is negatively charged (the spin-doublet state).

(3) The dimer is positively charged (the spin-doublet state).

Starting from the unreconstructed structure shown in Fig. 1(b), we calculated the optimized geometry by the energy-gradient method, where all the hydrogen atoms and seven underlayer Si atoms were fixed at their initial positions and only two Si atoms on the top surface were allowed to move freely.

III. RESULTS AND DISCUSSION

A. Atomic configurations

Figures 2(a)–2(d) show atomic configurations obtained for all cases at their most stable structures on the potential-energy hypersurfaces. These results clearly indicate that a symmetric dimer is formed in the electrically neutral case independent of the spin state. In contrast, a buckled dimer is formed in the negatively and the positively charged cases. Thus, we can conclude that a dimer buckles on the Si(001) surfaces at the parts where the electrical charge is not uniform.

In the neutral singlet state [Fig. 2(a)], the Si-Si distance of the dimer is 2.24 Å. On the other hand, the distance becomes 2.55 Å in the neutral triplet state [Fig. 2(b)]. On the buckled dimers, the difference in vertical height between Si atoms is 0.33 Å in the negatively charged case and 0.25 Å in the positively charged case. The Si-Si dis-

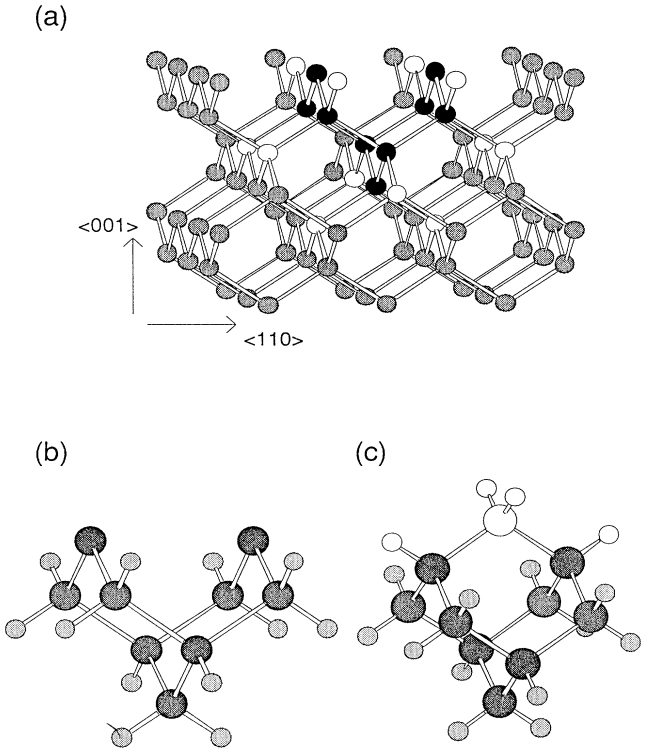

FIG. 1. (a) Si(001) unreconstructed (1×1) surface. Solid and open circles denote the parts considered. (b) The model molecular system produced from (a) and (c). Large and small spheres denote silicon and hydrogen atoms, respectively. (c) The optimized adamantane structure used for the determination of the structure (b).

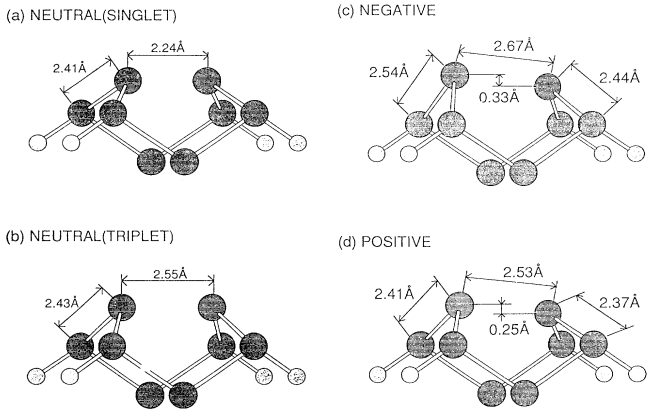

FIG. 2. (a) The most stable atomic configurations for the electrically neutral dimers in the singlet state, (b) in the triplet state, (c) the negatively charged dimer, and (d) the positively charged dimer. Five atoms located at the bottom part and four hydrogen atoms bonding to the second-layer Si atoms are omitted [cf. Fig. 1(b)].

tances become 2.67 and 2.53 Å, respectively, for the buckled dimers [Figs. 2(c) and 2(d)].

B. Electronic structures

The MO energy diagrams are shown in Fig. 3 for the symmetric dimer in the singlet state, the positively charged buckled dimer, and the negatively charged buckled dimer. It is noted that the degenerated energy levels for the α-spin and the β-spin electrons in the singlet symmetric dimer split into the corresponding different energy levels for those in the positively and negatively charged buckled dimers. In particular, the highest occupied MO (HOMO) of the singlet symmetric dimer splits into the HOMO and the lowest unoccupied MO (LUMO) in the positively charged buckled dimer, while the LUMO of the singlet symmetric dimer splits into the HOMO and the Xth MO in the negatively charged buckled dimer. A similar energy-level splitting takes place in the case of the symmetric dimer in the triplet state (see Fig. 2 in Ref. 22). These descending and ascending MO energy levels are generally observed when an electron is added to and eliminated from a molecule, respectively.

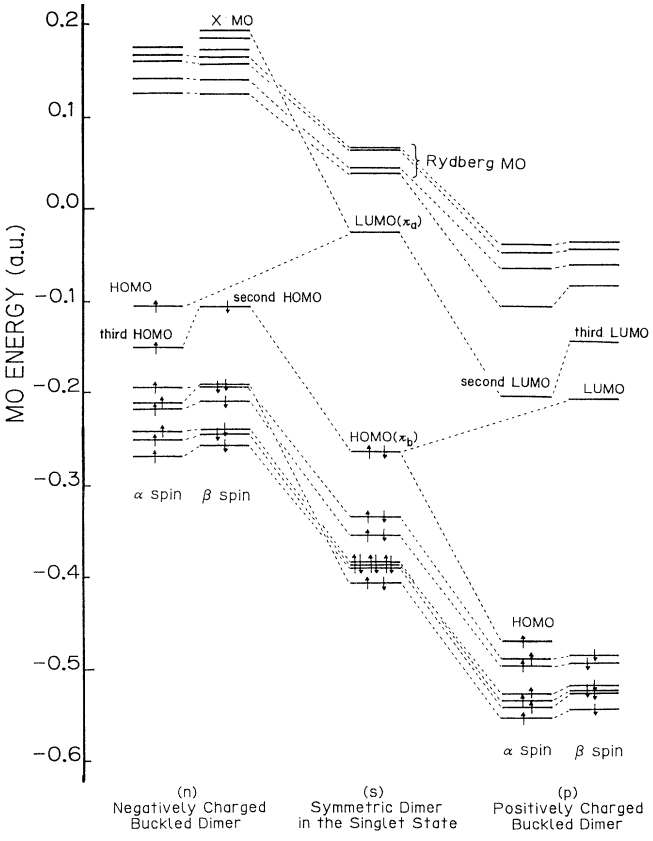

FIG. 3. (a) Molecular-orbital energy-level diagrams for the singlet symmetric dimer (s), the negatively charged buckled dimers (n), and the positively charged buckled dimers (p).

The electron density maps of MO's are collected in Fig. 4. The HOMO($s-1$) and the LUMO($s-2$) of the singlet symmetric dimer have π bonding (π_b) and antibonding (π_a) character, respectively. The HOMO($t-2$) and the second HOMO($t-1$) of the triplet symmetric dimer hold their character in the singlet state; i.e., the former ($t-2$) and the latter ($t-1$) originate from the LUMO($s-2$) and the HOMO($s-1$) of the singlet symmetric dimer, respectively. A remarkable feature is observed in both of the positively and negatively charged buckled dimers where the electron density in the MO is localized on one side of the Si atoms in the dimers (Fig. 4). Contrary to these situations, no such localization of the electron density in MO is found in the symmetric dimers in the singlet and the triplet states. The results of total electron density (the Mulliken population[18]) analyses and spin-density analyses are clearly explained from these figures.

The Mulliken population analysis (Fig. 5) indicates that the electron transfer from the "down" atom to the "up" atom is 0.42 electrons in both the negatively and positively charged buckled dimers. Chadi reported a similar electron transfer of 0.36 electrons. From Figs. 3 and 4, one can see that the HOMO of the positively charged buckled dimer is occupied by the unpaired extra α-spin electron, whose density is localized on the "up" atom in the HOMO ($p-1$). The same situation is observed in the negatively charged buckled dimer, where the unpaired extra electron density is localized on the "up" atom in the HOMO($n-3$). This is the origin of the electron transfer from the "down" atom to the "up" atom in the buckled dimers, irrespective of the positive or the negative charging.

The spin-density analysis (Fig. 5) shows that two unpaired α electrons in the triplet state are localized at the dimer part and are distributed symmetrically to the two Si atoms. These α electrons form the two dangling bonds on the dimer in the triplet state. However, the meaning of this dangling bond is not so simple as the usual σ-type dangling bond. As shown in Fig. 4, one of the two α electrons occupies the bonding π_b MO($t-1$), and the other α electron occupied the antibonding π_a MO($t-2$). It should be noted that both the π_b and π_a are completely delocalized over the dimer.

In the buckled dimer, the unpaired α electron exists on the "down" atom in the negatively charged case [Fig. 5(c)], but on the "up" atom in the positively charged case [Fig. 5(d)]. These complicated results are clearly explained by using Figs. 3 and 4. The second ($n-2$) and the third ($n-1$) HOMO's of the negatively charged buckled dimers originate from the HOMO ($s-1$) of the symmetric dimers. The second HOMO ($n-2$) is occupied by the β electron localized on the "up" atom and the third HOMO($n-1$) is occupied by the α electron localized on the "down" atom. Since the α electron in the HOMO($n-3$) and the β electron in the second HOMO($n-2$) cancel each other out, the spin density on the "up" atom vanishes. In this way the α electron in the third HOMO($n-1$) localized on the "down" atom is observed as a net spin density in the negatively charged

buckled dimers. On the other hand, the α-spin density in the positively charged buckled dimer is described by the unpaired α-electron density in the HOMO($p-1$).

Total electron-density maps for the nonbuckled and the buckled dimers are illustrated in Fig. 6. It is noted that a considerably strong bond is generated between two Si atoms in the dimer for all cases. The total electron-density distributions in Figs. 6(a) and 6(b) seem to reflect the STM image for the symmetric dimer, where the dimer has a twin bean-shaped image. Those of Figs. 6(c) and 6(d), however, do not explain the STM image for the buckled dimer, where the "up" atom is bright and the "down" atom is dark. On the other hand, the electron-density distributions of the molecular orbitals shown in

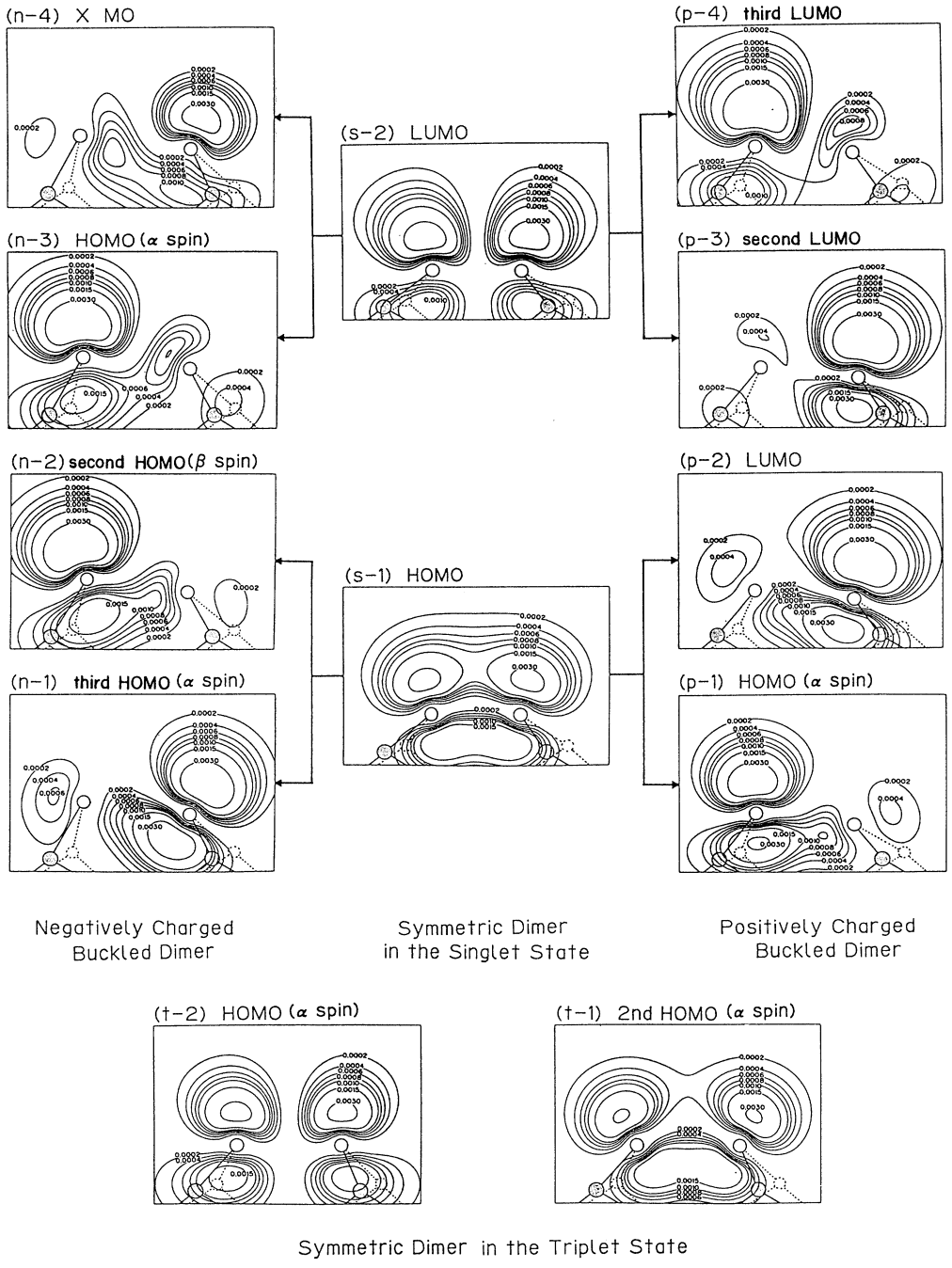

FIG. 4. Contour plots of the electron-density distributions of the molecular orbitals for the symmetric dimers in (a) the singlet (center) and (b) the triplet states (lower), and for the buckled dimers charged (c) negatively (left) and (d) positively (right). These are plotted on the (110) plane shown in Fig. 1(a) in units of e/bohr^3.

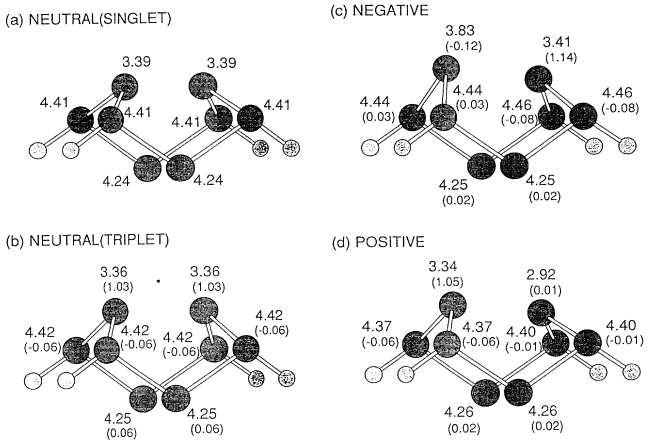

FIG. 5. Electron densities and spin densities (shown in parentheses) obtained by the Mulliken population analysis on the symmetric dimers in (a) the singlet and (b) the triplet states, and on the buckled dimers charged (c) negatively and (d) positively. Five atoms located at the bottom part and four hydrogen atoms bonding to the second-layer Si atoms are omitted [cf. Fig. 1(b)].

Fig. 4 express well the characteristic of both STM images. Research will be extended on this point in the following paper.[22]

C. Comparison with STM experiments

Tromp *et al.* made it clear by STM photographs[15,16] that buckled dimers are formed only in the vicinity of dimer defects or step edges. The asymmetric structures of defects or steps may produce unbalanced charge distributions on the surface.

From our theoretical results, the "up" atom is more negatively charged than the "down" atom in the buckled dimer. This imbalance of charge distribution in the dimer influences the adjacent dimers. In other words, the buckled dimer inflicts an asymmetric Coulomb potential on the adjacent dimer. When the adjacent dimer also buckles, the negative charges on both "up" atoms repulse each other and the two "up" atoms move to make the distance as far as possible. This situation means that the opposite-side atoms of the adjacent dimers will rise up and a zigzag dimer row will be produced. This may be a secondary factor to induce the buckling itself.

LEED,[2,3] He diffraction,[4] and ARUPS (Refs. 9–11) exhibit the existence of other reconstructions, $c(4\times2)$

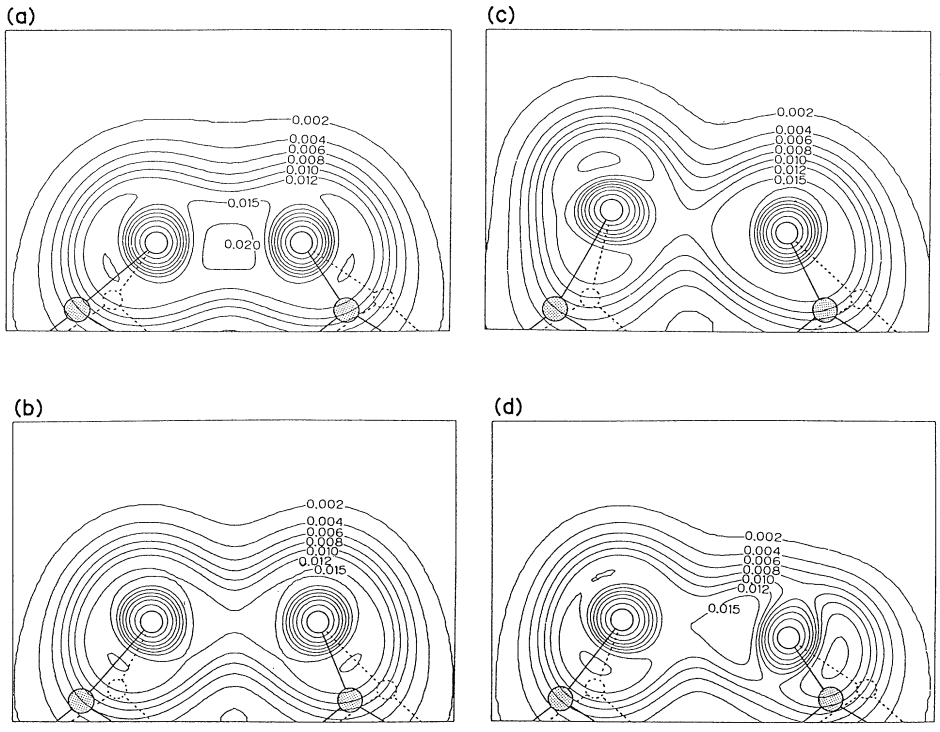

FIG. 6. Contour plots of the total electron-density distribution for the symmetric dimers in (a) the singlet and (b) the triplet states, and for the buckled dimers charged (c) negatively and (d) positively. These are plotted on the (110) plane shown in Fig. 1(a) in units of e/bohr^3.

and $p(2\times2)$, in addition to the fundamental (2×1) structure. The structure made by two zigzag dimer rows in parallel is just $c(4\times2)$ or $p(2\times2)$. When the Si(001) surface has many defects, $c(4\times2)$ or $p(2\times2)$ structure is spread more widely on the surface and the intensity of LEED signals will become stronger, whereas the well-prepared clean surface is electrically neutral and mainly occupied by nonbuckled (2×1) structure.

A recent experiment with STM (Ref. 23) performed by Sakurai *et al.* also supports our theoretical results. They prepared a clean Si(001)-(2×1) surface, and then let alkali-metal atoms (Li or K) be adsorbed to the surface. The STM topograph showed that a zigzag pattern of buckled dimers was formed around the adsorbed alkali atom, whereas symmetric dimers remained in the other place. A reasonable explanation shall be given by our theoretical result. Alkali atoms are ionized easily in the following manner due to the low ionization potential:

$$\mathrm{Li}\rightarrow\mathrm{Li}^{+}+e^{-}\ ,$$

$$\mathrm{K}\rightarrow\mathrm{K}^{+}+e^{-}\ .$$

The electron released from the adsorbed alkali atom will be transferred to the surface; i.e., Si atoms have excessive electrons near the adsorbate. This situation can make the dimers buckled.

IV. CONCLUSION

It was clarified by the *ab initio* quantum chemical calculations that the two types of dimer structure, buckled and nonbuckled, found on the Si(001) surface are caused by the local electrical charge distribution on the surface. The dimer is symmetric when there is no excess electric charge, whereas the dimer is buckled where there is an unbalanced electrical charge. These theoretical results are consistent with the recent STM observations and account clearly for the origin of the buckling in the dimer formation on reconstructed Si(001) surfaces.

ACKNOWLEDGMENTS

This work was partially supported by a Grant-in-Aid for Scientific Research on Priority Areas, Metal-Semiconductor Surface, from the Ministry of Education, Science and Culture (No. 02232106). The authors thank the Computer Center, Institute for Molecular Science, Okazaki, for the use of the M680H/S-820 computer system and the Library program GAUSSIAN82. The computations were also carried out at the Computer Center, the University of Tokyo, and the Computer Center, Chiba University.

[1]S. J. White and D. P. Woodruff, Surf. Sci. **64**, 131 (1977).
[2]T. D. Poppendieck, T. C. Ngoc, and M. B. Webb, Surf. Sci. **75**, 287 (1978).
[3]T. Tabata, T. Aruga, and Y. Murata, Surf. Sci. **179**, L63 (1987).
[4]M. J. Cardillo and G. E. Becker, Phys. Rev. B **21**, 1497 (1980).
[5]D. J. Chadi, Phys. Rev. Lett. **43**, 43 (1979).
[6]D. J. Chadi, Phys. Rev. Lett. **41**, 1062 (1978).
[7]M. T. Yin and M. L. Cohen, Phys. Rev. B **24**, 2303 (1981).
[8]W. S. Verwoerd, Surf. Sci. **99**, 581 (1980).
[9]H. A. Van Hoof and M. J. Van Der Wiel, Appl. Surf. Sci. **6**, 444 (1980).
[10]H. H. Farrell, F. Stucki, J. Anderson, D.J. Frankel, G. J. Lapeyre, and M. Levinson, Phys. Rev. B **30**, 721 (1984).
[11]R. I. G. Uhrberg, G. V. Hansson, J. M. Nicholls, and S. A. Flodstrom, Phys. Rev. B **24**, 4684 (1981).
[12]F. J. Himpsel and Th. Fauster, J. Vac. Sci. Technol. A **2**, 815 (1983).
[13]E. Artacho and F. Yndurain, Phys. Rev. Lett. **62**, 2491 (1989).
[14]A. Redondo and W. A. Goddard III, J. Vac. Sci. Technol. **21**, 344 (1982).
[15]R. M. Tromp, R. J. Hamers, and J. E. Demuth, Phys. Rev. Lett. **55**, 1303 (1985).
[16]R. J. Hamers, Ph. Avouris, and F. Bozso, Phys. Rev. Lett. **59**, 2071 (1987).
[17]R. J. Hamers, Ph. Avouris, and F. Bozso, J. Vac. Sci. Technol. A **6**, 508 (1988).
[18]See, for example, A. Szabo and N. S. Ostlund, *Modern Quantum Chemistry* (MacMillan, London, 1982).
[19]W. R. Wadt and P. J. Hay, J. Chem. Phys. **82**, 284 (1985).
[20]M. S. Gordon, J. Chem. Phys. **69**, 4955 (1978).
[21]J. S. Binkley, M. Frisch, D. J. DeFrees, K. Raghavachari, R. A. Whiteside, H. B. Schlegel, G. Flueter, and J. A. Pople, GAUSSIAN82 (Carnegie-Mellon Chemistry Publication Unit, Pittsburgh, 1983).
[22]T. Hoshino, S. Oikawa, M. Tsuda, I. Ohdomari, following paper, Phys. Rev. B **44**, 11 248 (1991).
[23]T. Hashizume, Y. Hasegawa, I. Kamiya, T. Ide, I. Sumita, S. Hyodo, and T. Sakurai, J. Vac. Sci. Technol. A **8**, 233 (1990).